Weierstraß-Institut

für Angewandte Analysis und Stochastik

Leibniz-Institut im Forschungsverbund Berlin e. V.

Preprint ISSN 0946 – 8633

Rogue wave formation by accelerated solitons at an optical event horizon

Ayhan Demircan,[1] Shalva Amiranashvili,[2] Carsten Brée,[2] Christoph Mahnke,[3]

Fedor Mitschke,[3] Günter Steinmeyer [4]

submitted: June 27, 2013

[1] Leibniz Universität Hannover
Welfengarten 1
30167 Hannover, Germany
E-Mail: demircan@iqo.uni-hannover.de

[2] Weierstraß-Institut
Mohrenstraße 39
10117 Berlin, Germany
E-Mail: Shalva.Amiranashvili@wias-berlin.de
E-Mail: Carsten.Bree@wias-berlin.de

[3] Institute for Physics
University of Rostock
Universitätsplatz 3
18055 Rostock, Germany
E-Mail: christoph.mahnke@uni-rostock.de
E-Mail: fedor.mitschke@uni-rostock.de

[4] Max Born Institute for Nonlinear Optics
and Short Pulse Spectroscopy
Max-Born-Straße 2A
12489 Berlin, Germany
Optoelectronics Research Centre
Tampere University of Technology
33101 Tampere, Finland
E-Mail: steinmey@mbi-berlin.de

No. 1807

Berlin 2013

2010 *Physics and Astronomy Classification Scheme.* 42.65.Re, 42.65.Ky, 42.65.Tg, 42.81.Dp.

Key words and phrases. Rogue wave, Optical soliton, Ultrashort pulse, Optical event horizon.

Acknowledgments. Sh.A. acknowledges support by the DFG Research Center MATHEON under project D 14, F.M. and C.M. by DFG, and G.S. by the Academy of Finland under project grant 128844.

Edited by
Weierstraß-Institut für Angewandte Analysis und Stochastik (WIAS)
Leibniz-Institut im Forschungsverbund Berlin e. V.
Mohrenstraße 39
10117 Berlin
Germany

Fax: +49 30 2044975
E-Mail: preprint@wias-berlin.de
World Wide Web: http://www.wias-berlin.de/

Abstract

Rogue waves, by definition, are rare events of extreme amplitude, but at the same time they are frequent in the sense that they can exist in a wide range of physical contexts. While many mechanisms have been demonstrated to explain the appearance of rogue waves in various specific systems, there is no known generic mechanism or general set of criteria shown to rule their appearance. Presupposing only the existence of a nonlinear Schrödinger-type equation together with a concave dispersion profile around a zero dispersion wavelength we demonstrate that solitons may experience acceleration and strong reshaping due to the interaction with continuum radiation, giving rise to extreme-value phenomena. The mechanism is independent of the optical Raman effect. A strong increase of the peak power is accompanied by a mild increase of the pulse energy and carrier frequency, whereas the photon number of the soliton remains practically constant. This reshaping mechanism is particularly robust and is naturally given in optics in the supercontinuum generation process.

1 Introduction

The appearance of waves with extreme amplitude has been observed in varous physical systems [1, 2, 3, 4, 5, 6, 7, 8]. Their appearance is most drastically illustrated for the case of ocean waves [9, 10, 11], with waves exceeding the average wave crest by a factor two or even more and causing serious damage to ocean-going ships. Recently, similar phenomena have also been reported in optics where extreme events were observed in the soliton-supporting red tail of supercontinua (SC) in fibers [6]. Substantial progress has also been made in the understanding of the mechanisms behind the optical rogue waves [12, 13, 14, 15]. Currently, most explanations follow one of two alternatives: solitons or breathers. The former involves soliton fission and selective Raman shifting of the largest solitons to the long-wavelength side of the spectrum [13, 14]. The latter builds on the dynamics of known special solutions of the propagation equation as Akhmediev breathers [15, 16] or the Peregrine soliton [17].

A different possibility has been demonstrated in [18], where rogue waves result from the unusual interaction of fundamental solitons with the low-level radiation background. The main mechanism refers to a reflection process between pulses that originates from the wave blocking effect in fluid dynamics [19]. In optics, it was first demonstrated as the “optical push broom effect” in a fiber Bragg grating [20]. The reflection of pulses has also been discussed in recent works on beam collisions [21, 22] and soliton trapping [23, 24]. In fact, this particular kind of the reflection process appears in many wave-supporting physical systems and may be interpreted as a simple analogue of the event horizon [25]. Moreover, the fiber-optical analogue of an event horizon [26, 27] requires only generic preconditions and can be understood in terms of the familiar cross

phase modulation (XPM) [28] between continuum radiation in the normal dispersion range and solitons. We will refer to the continuum radiation as dispersive wave (DW).

For our approach, it is crucial that event horizon analogues appear together with the rogue waves both in fibers [29, 30, 31] and for water waves [32]. The same photonic crystal fiber used for the experimental verification of an optical event horizon [26] has been shown to exhibit optical rogue waves [14]. The reason is that the conditions for all-optical reflection at an optical event horizon are inherently given in the SC process [18, 24, 33]. However, the highly complex SC generation involves several types of collision processes. In particular, soliton fusion and multiple collisions between solitons can be observed, which appear superimposed on a low-level radiation background. As soliton-soliton collisions can lead to the emergence of a so-called "champion soliton" [34] and have been shown to contribute to the formation of optical rogue waves [35], it is important to separate the contributions of different processes.

In the following, we demonstrate a typical SC generation scenario leading to one giant soliton that appears even before the first binary collision between solitons takes place. Its emergence can clearly be identified as resulting from the interaction between the soliton and DWs. The resulting giant soliton posses all generic features of rogue waves.

2 Propagation model for the SC generation

It has been shown that the standard nonlinear Schrödinger equation, describing self-phase modulation and second -order dispersion and including only the additional effect of third-order dispersion, suffices to observe rogue waves in the SC generation process [35]. However, the rogue waves are generated by interactions of ultrashort few-cycle pulses. The latter are accurately described beyond the standard treatment with an envelope approximation. In addition, the investigations of dramatic concentration of energy into a rogue wave initiated by DWs presuppose a correct modeling of nonlinear processes between spectrally disparate waves and the energy transfer between them. To derive such a basic propagation equation for the real-valued optical field $E(z,t)$, e.g., in a single-mode fiber with the propagation constant $\beta(\omega)$, it is convenient to introduce a complex-valued $\mathcal{E}(z,t)$ such that in the frequency domain

$$\mathcal{E}_\omega(z) = E_\omega(z) - \frac{i\partial_z E_\omega(z)}{|\beta(\omega)|}. \tag{1}$$

Note that $E = \mathrm{Re}[\mathcal{E}]$. The definition (1) can be understood by considering a linear superposition of forward waves

$$E(z,t) = \sum_\omega A_\omega e^{i[\beta(\omega)z-\omega t]}, \qquad A_{-\omega} = A_\omega^*$$

for which one immediately obtains

$$\mathcal{E}(z,t) = 2\sum_{\omega>0} A_\omega e^{i[\beta(\omega)z-\omega t]}.$$

Therefore the complex field contains only positive frequencies for the forward propagation. In this formulation the negative-frequency part of $\mathcal{E}(z,t)$ corresponds to the backward waves. In

the unidirectional approximation, $\mathcal{E}(z,t)$ is closely related to the analytic signal for the electric field $\mathcal{E}(z,t) = 2\sum_{\omega>0} E_\omega(z)e^{-i\omega t}$ and thus to the pulse envelope. In general, $\mathcal{E}(z,t)$ describes both forward and backward waves, which are mutually coupled by nonlinear interaction. Moreover, expressing, e.g., a cubic nonlinear term in terms of the complex field, one sees that contributions of the different four-wave mixing processes are now separated. For a favorable dispersion profile $\beta(\omega)$ one can then omit higher harmonic generation without any reference to the carrier frequency and the slowly varying envelope approximation.

The basic propagation equation for $\mathcal{E}(z,t)$ in a Kerr medium reads [36, 37]

$$i\partial_z \mathcal{E}_\omega + |\beta(\omega)|\mathcal{E}_\omega + \frac{3\omega^2\chi^{(3)}}{8c^2|\beta(\omega)|}(|\mathcal{E}|^2\mathcal{E})_\omega = 0, \tag{2}$$

and possesses many useful features of the nonlinear Schrödinger equation while being bidirectional. Parameters c and $\chi^{(3)}$ are the speed of light and the third-order nonlinear susceptibility, respectively. For unidirectional propagation only the positive-frequency part of $|\mathcal{E}|^2\mathcal{E}$ contributes to Eq. (2). The latter is then equivalent to the unidirectional forward Maxwell equation [38], but with the benefit of a clear separation of third-harmonic generation terms.

The fiber propagation constant may be obtained by numerical integration of the group delay $\beta_1(\omega) = \beta'(\omega)$ and then approximated following [39]. Figure 1 depicts an exemplary group delay $\beta_1 = \beta'(\omega)$ and related group-velocity dispersion $\beta_2 = \beta''(\omega)$ of a photonic crystal fiber. The presence of absorptive resonances in the ultraviolet as well as vibrational resonances in the infrared causes a characteristic concave group-velocity dispersion profile with a ZDW located at $0.87\,\mu$m wavelength, which may appear shifted due to waveguide dispersion effects. In our simulations, dispersive properties are described by $\beta(\omega) = n(\omega)\omega/c$, where the refractive index $n(\omega)$ is approximated by a suitable rational function. The chosen rational representation leads to a physically correct approximation of chromatic dispersion throughout the transparent region of dielectric media [39].

Equation (2) is subject to the conservation laws

$$I_1 = \sum_\omega \frac{n(\omega)}{\omega}|\mathcal{E}_\omega|^2, \qquad I_2 = \sum_\omega n(\omega)|\mathcal{E}_\omega|^2 \tag{3}$$

where $I_{1,2}$ are finite and proportional to the time-averaged photon flux and power, respectively [36]. Our approach correctly models nonlinear processes between spectrally disparate waves, i.e., four-wave mixing processes and XPM between solitons and DW as well as between individual solitons. If the slow envelope description with respect to a carrier frequency ω_0 applies, Eq. (2) reduces to the standard nonlinear Schrödinger equation [28] with the nonlinearity parameter $\gamma = (3\omega_0\chi^{(3)})/[4\epsilon_0 c^2 n^2(\omega_0)A_{\text{eff}}]$, where A_{eff} is the effective fiber area.

For our numerics we use either a de-aliased pseudospectral method, with the implementation of the Runge-Kutta integration scheme in the frequency domain and adaptive step-size control, or a more direct split-step Fourier approach with sufficiently small fixed steps. The numerics are controlled by tracing the integrals of motion. Quality of the time discretization is ensured by exemplary runs with the considerably larger number of harmonics.

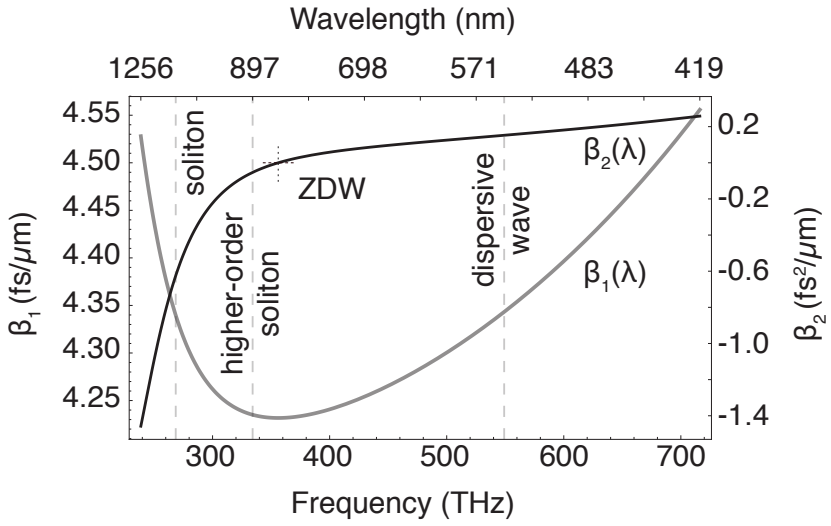

Figure 1: Concave group delay $\beta_1 = \beta'(\omega)$ and related group-velocity dispersion $\beta_2 = \beta''(\omega)$, with the extracted wavelengths for the initial higher-order soliton at $\lambda_s = 897\,\text{nm}$, one ejected fundamental soliton at $\lambda_s = 1030\,\text{nm}$ and a dispersive pulse at $\lambda_d = 614\,\text{nm}$ (vertical dashed lines).

3 Accelerated solitons in the supercontinuum generation

For investigations of the SC, we launch a hyperbolic secant pulse (center wavelength $897\,\text{nm}$) into the anomalous dispersion regime of the fiber close to the ZDW $= 842\,\text{nm}$. Figure 2 show the evolution of the SC in the time domain for soliton orders $N = 74$ and $N = 111$. For a nonlinear fiber with $\gamma = 0.1\,\text{W}^{-1}\text{m}^{-1}$ these correspond to a peak power of $54\,\text{kW}$ and $96\,\text{kW}$ respectively. In all cases the formation of the SC involves soliton fission [38] and modulation instability [40], ensuring the increase of the initial spectral width by one to two orders of magnitude [41].

Figure 2 illustrates the decay of two high-order solitons in the presence of third-order dispersion, leading to a multitude of fundamental soliton trajectories after millimeters of propagation length. This process has also been termed soliton fission [38]. In Fig. 2 the soliton trajectories stand out against the low-power dispersive background as temporally highly confined regions of high peak intensity, which are marked yellow or orange. If undisturbed, the soliton trajectories should appear as straight lines in the z-t plane, with a slope dictated by their group velocity. While inspection of Fig. 2 reveals many undisturbed soliton trajectories, there also appear curved ones, which are indicative of soliton acceleration (concave) or deceleration (convex). Some of these characteristic trajectory bends are obviously caused by soliton collisions.

The acceleration of solitons in the SC can also be observed under the influence of the Raman effect [33]. The related soliton fusion process or, more generally, multiple collisions between solitons have been suggested as a possible driver mechanism behind rogue waves [42, 35]. This mechanism is based on the emergence of a so-called “champion soliton” in a nearly integrable system close to the standard nonlinear Schrödinger equation [34], where a high number of fundamental solitons undergoes turbulent collisions. In the SC process, giant solitons are

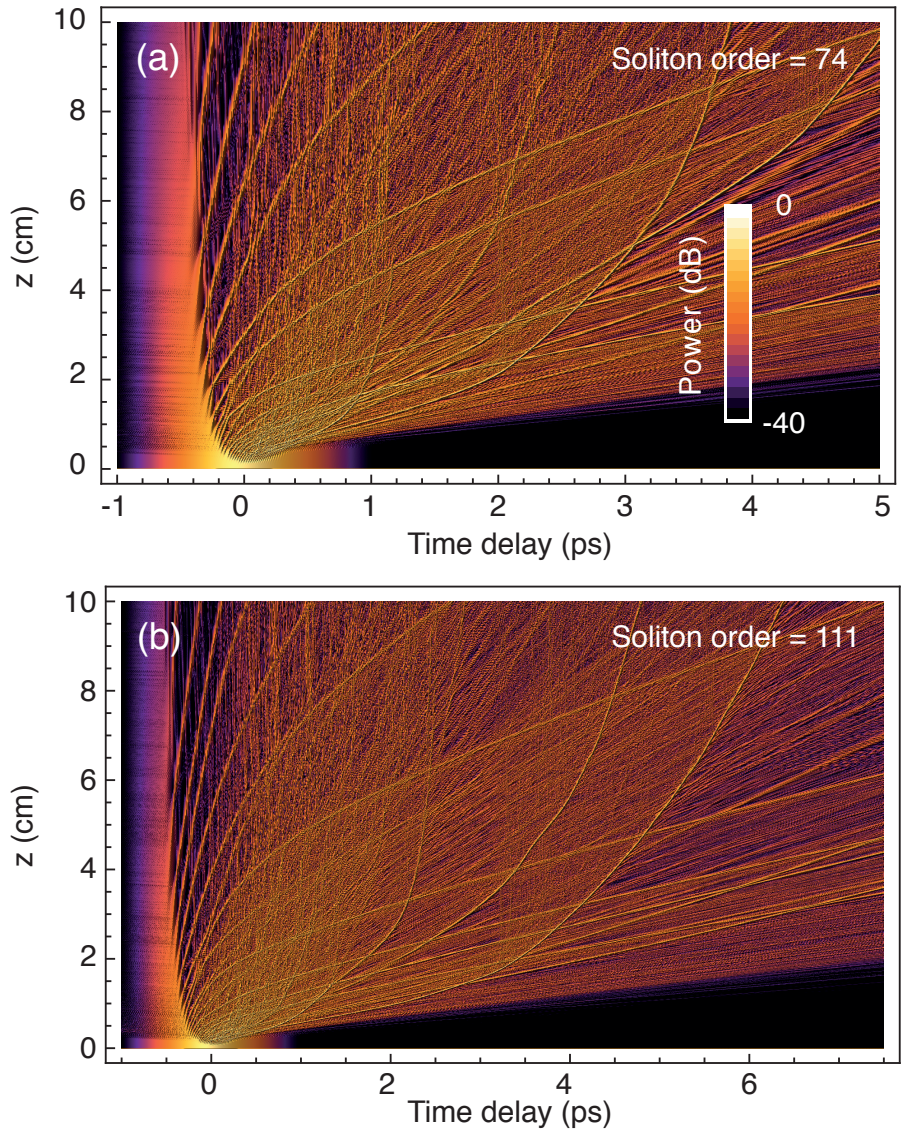

Figure 2: Temporal evolution of $|\mathcal{E}(z,t)|^2$ of a higher-order soliton injected close to the ZDW into the fiber along z for a typical SC generation process by soliton fission for the soliton order (a) $N = 74$ and (b) $N = 111$. Note that the calculation does not involve the Raman effect.

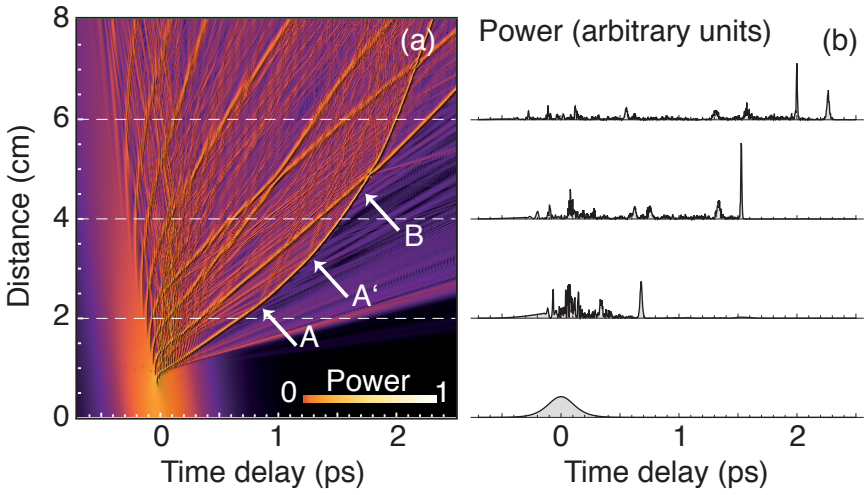

Figure 3: (a) Temporal evolution of $|\mathcal{E}(z,t)|^2$ of a higher-order soliton along z for a SC generation for $N = 28$. (b) Cross sections for selected z-values.

observed after only a few such collision processes. However, a mechanism which could explain rogue wave observations solely by soliton collisions could not be identified up to now. In [18] another collision process inherently present in the SC process has been demonstrated. This mechanism has the ability of significantly increasing the peak power of solitons and results from the interaction between the dispersive continuum background and the particular solitons. Their mutual interaction leads to the acceleration of the soliton, which is accompanied by the generation of transient giant waves, fulfilling three main criteria for rogue waves [43]. The interaction of the soliton with the dispersive radiation is accompanied by soliton-soliton collisions, which may further manipulate soliton properties. Although any trajectory of the solitons can be traced back in the numerical data, it is still difficult to irrefutably pinpoint the rogue wave generation mechanism in the statistical data. However, Fig. 2 already reveals an important characteristics of the newly suggested rogue wave generation mechanism. In both examples, the soliton acceleration starts in an advanced stage of the SC, clearly isolated from the early very dense interaction scenario during the initial soliton decay.

4 Rogue waves by low soliton orders

To gain deeper insight into the part of the interaction process that is independent of soliton-soliton collisions, we performed calculations at lower soliton numbers. Figure 3 represents a SC generated by a soliton of order $N = 28$. The reduction to much fewer fundamental solitons ejected by the fission process allows the generation of only one giant wave in the SC, without any collision with other solitons.

Figure 3 shows the typical SC evolution in the time domain. With the rather moderate peak power in this example, the impact of modulation instability can be neglected [44]. The fundamental solitons produced in the fission process exhibit durations between 10 and 20 fs with different peak powers, appearing as pronounced lines that clearly stand out from the background.

The fission process also generates DWs in the normal dispersion regime [38, 41]. The further away from the zero-dispersion wavelength the solitons are being generated, the slower they will propagate [44], accumulating delay (Fig. 3). As we deliberately excluded Raman scattering in our analysis, we observe the same propagation dynamics as in [18], with the noted exception that only one accelerated soliton is generated and that soliton-soliton scattering is reduced. In fact, inspection of Fig. 3 reveals that the trajectory of this soliton cannot be influenced by rare isolated scattering events within the segment $\overline{\mathrm{AB}}$. In this case, the physical mechanisms behind this peculiar acceleration and the accompanied increase of the peak power appears clearly isolated from competing processes, without the problem of superposition of different mechanisms.

We numerically isolated the soliton, separated it from accompanying continuum radiation, and fitted the model function $f(t) = P_0 \operatorname{sech}^2[(t-t_*)/t_0]$ to its intensity envelope (Fig. 4, FWHM $= 1.76t_0$). Compared to the steady propagation at $z < 2.2$ cm, Fig. 4(a) confirms a deviation of $t_*(z)$ from the initial linear trajectory by -600 fs at point B ($z = 4.5$ cm). This temporal shift is accompanied by approximately 4 % change of pulse energy $\propto I_2$ and by a more than twofold increase of peak power $P_0(z)$, [solid and dashed curves in Fig. 4(b), respectively]. Pulse duration scales accordingly from an initial 20 fs (FWHM) to sub-10 fs at B. Furthermore, a Fourier analysis indicates that the center wavelength $\lambda_0(z)$ of the soliton shifts from 1060 to 985 nm within the 2.3 cm propagation from A to B, reflecting the according energy transfer.

Under similar conditions, the impenetrability of the soliton trajectory was referred to as an optical event horizon for the DW [26]. In [45] it has been shown how the interaction at the optical event horizon and the accompanied frequency shift of the soliton can be exploited for an efficient manipulation of a strong signal pulse by a weak DW. Here we have the same situation occurring between two small portions of a SC in a photonic crystal fiber, with a lot of unrelated dynamics happening at the same time.

Rogue waves, subject to non-Gaussian statistics, have previously been shown to appear in the fiber SC generation without Raman frequency shift in [35], where rogue events have been related to multiple collisions between optical solitons. In our case, however, there is no other soliton anywhere close between A to B. Therefore, appearance of a rogue wave can only be explained by nonlinear continuum-soliton interaction. Namely, for each soliton velocity there is a spectral slice of dispersive non-solitonic radiation that propagates at nearly identical group velocity. Group-velocity matching significantly increases the nonlinear interaction length between continuum and soliton and may lead to significant reshaping of the latter. Comparing to the energy of the DW within temporal overlap with the soliton [dotted line in Fig. 4(b)], it is striking that changes of any of the soliton parameters $t_*(z)$, $\lambda_0(z)$, and $P_0(z)$ are strongly correlated with the strength of the DW, see positions A and A' marked in Figs. 3–4.

5 Controlled generation of giant waves

For further investigation of this scenario, we numerically isolated the primary soliton and selected segments of the DW in Fig. 3(a) right at the onset of the trajectory curvature, making a deterministic interpretation of the acceleration process of the soliton uncoupled from the SC generation process possible. To this end, we inject into the fiber a fundamental soliton at

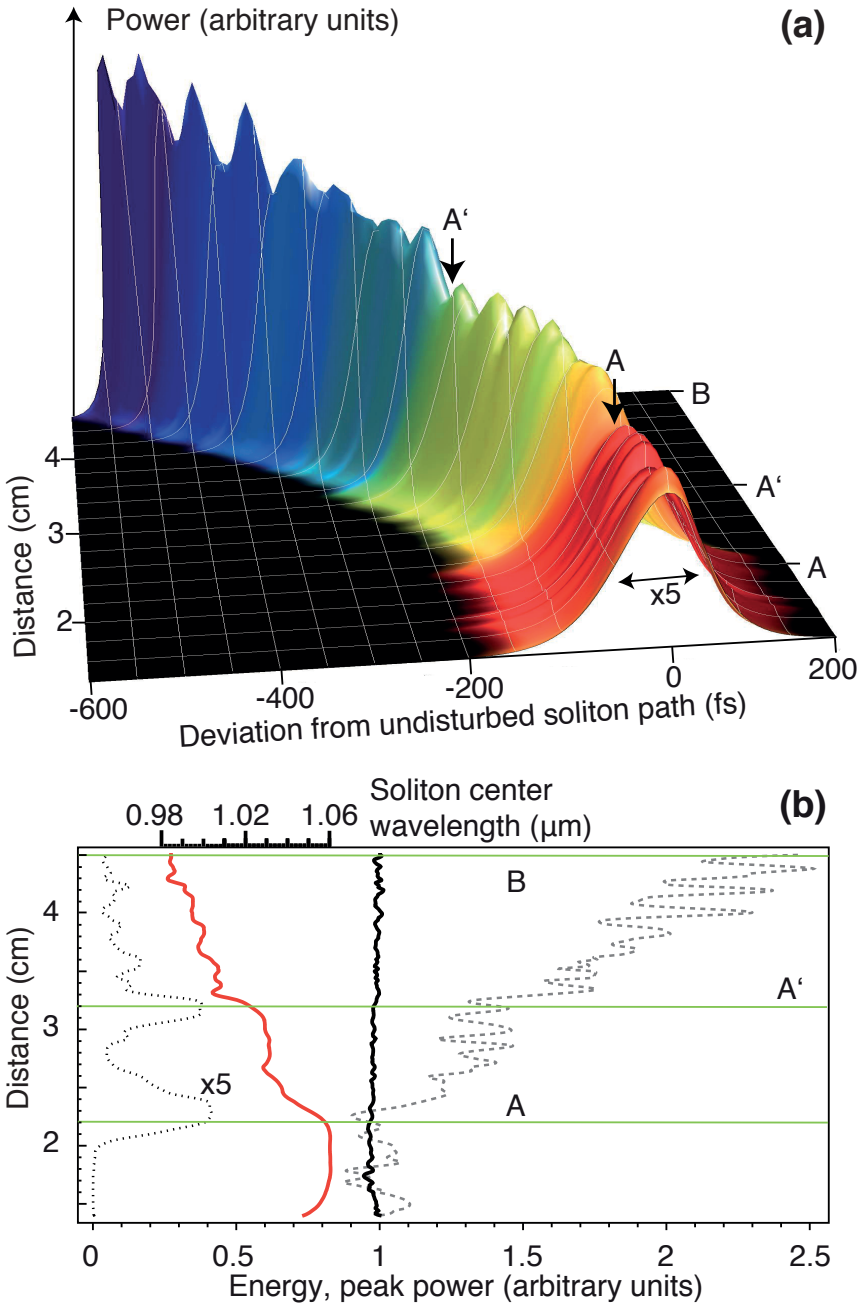

Figure 4: (a) Visualization of the soliton propagating from A to B in Fig. 3. Temporal delays are shown relative to the unperturbed propagation of the soliton at $z = 1.5$–2 cm. For clarity, the width of the soliton has been stretched by a factor 5. Color coding visualizes $\lambda_0(z)$, which changes from 1060 to 985 nm (red and blue, respectively). (b) Development of soliton parameters $\lambda_0(z)$ (thick red line), pulse energy $\propto I_2$ (solid black line), and peak power $P_0(z)$ (dashed line). Energy content of the DW within $\pm 1.5\tau$ interval around $t_*(z)$ is shown as a dotted line.

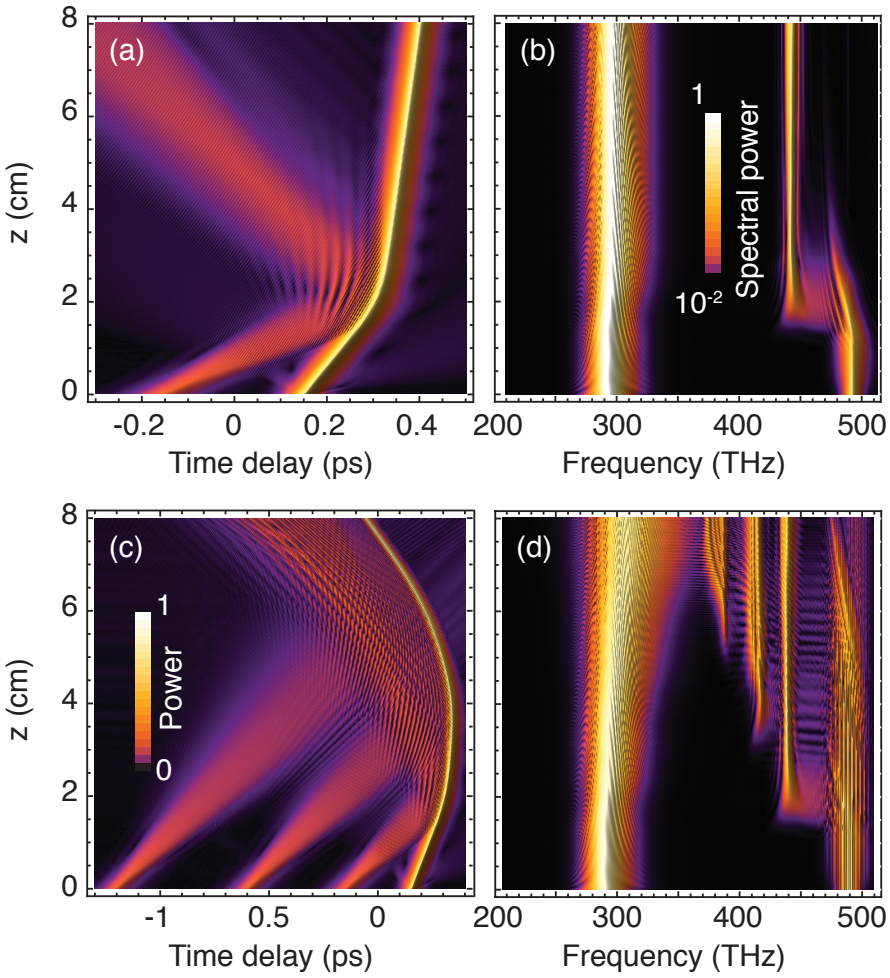

Figure 5: Time domain (a) and spectral (b) evolution along the fiber with a fundamental soliton at $\lambda_s = 1.03\,\mu$m and a dispersive pulse at $\lambda_d = 0.614\,\mu$m, representing a typical scattering process of a DW at an optical horizon at the edge of a soliton. (c) and (d) the same for cascaded scattering with three dispersive pulses at $\lambda_d = 0.614\,\mu$m.

$\lambda_s = 1030\,$nm of $26.6\,$fs FWHM duration together with slightly slower propagating $53.2\,$fs time segments of DWs near the velocity-matched wavelength of $\lambda_d = 614\,$nm. The extracted parameters fulfill the necessary conditions to induce a small yet sufficient increase of the refractive index by the soliton to build up an optical event horizon for the DW [26, 45].

In a suitable reference frame, Fig. 5(a) illustrates a scattering process of a DW at the propagation front of a soliton in the time domain, a process that has previously been dubbed as “reflection in the event horizon” [26]. The main point here is a strong reshaping of both, the soliton and the DW, in contrast to the standard setup of reflection process, where only the weak pulse changes its properties [20, 21, 22, 23]. Figure 5(b) elucidates the identical situation in the spectral domain, leading to a slight blue shift of the soliton together with a more pronounced red shift of the DW. However, the properties of the fundamental soliton are only slightly changed. To amplify the manipulation of the soliton, we increase the number of DWs and simulate a scattering process between three DWs and a soliton [Fig. 5(c,d)].

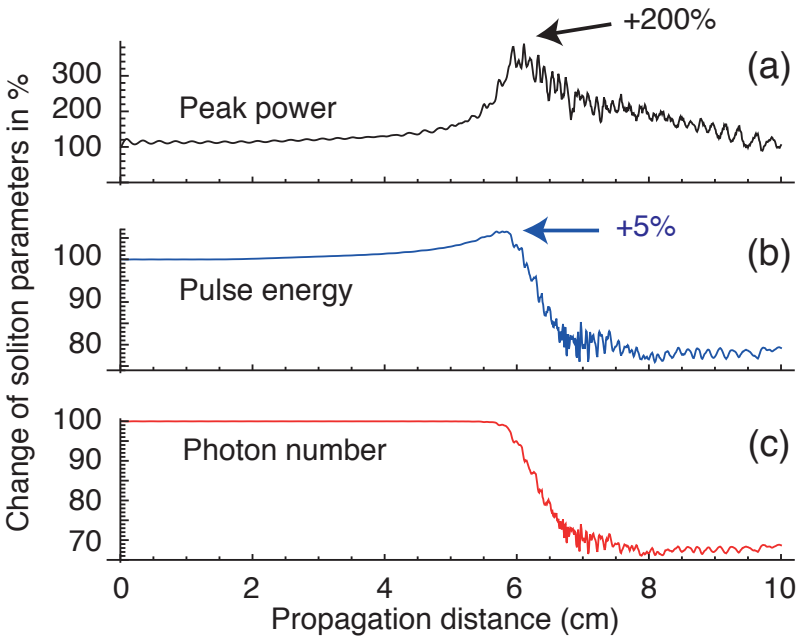

Figure 6: Relative change of soliton parameters by the interaction with three segments of the resonant DW as shown in Figs. 5(c,d). (a) Peak power, (b) energy, (c) photon number defined by Eq. (3) (see [36]).

Compared to a single scattering event, a nearly threefold increase is thereby achieved. Consequently, throughout the scattering processes, the soliton experiences a further increase of its group velocity, resulting in an accelerated trajectory, as is also observed in the SC generation [Fig. 3(a)]. In the frequency domain, each scattering event further shifts the soliton towards shorter wavelengths [Fig. 5(d)], with an opposite effect on the non-solitonic continuum radiation.

The relative change of all soliton parameters by the interaction process with the DW is shown in Fig. 6. In particular, it is reassuring that the photon number of the soliton (red line) is practically conserved in this process. Consequently, a slight increase of the soliton energy (blue line) results from the frequency shift of the soliton center frequency towards higher values. In contrast to these rather mild changes of pulse energy and photon number, there is a pronounced increase of peak power (black line). Given the rather small frequency shift of the soliton, such a dramatic effect can only result from the strong dependence of the soliton properties from the dispersion value. The frequency-shifted soliton experiences a considerably smaller β_2 (Fig. 1) than the input pulse. Considering that the energy of a soliton is connected to the peak power P_0 and β_2 via $E = 2\sqrt{P_0|\beta_2|/\gamma}$, the decrease of β_2 cannot be compensated by a reduction of E as E grows, too. As γ does not vary appreciably, consequently, P_0 is forced to grow massively, depending on the variation of β_2. The stronger the frequency shift, therefore, the smaller β_2-values can be achieved.

We repeated these simulations with several segments of continuum radiation. Figure 7 shows the fundamental soliton after the collision with 3, 6, and 9 wave packets, resulting in an up to threefold increase of the soliton peak power. The soliton peak power and temporal width strongly depend on the pulse parameters of the DW [45], and even higher soliton peak powers can be

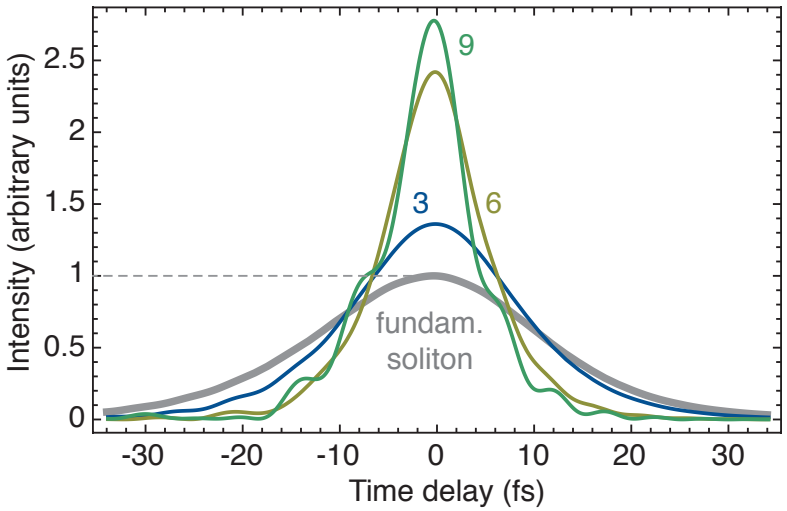

Figure 7: Enhanced peak power after collision: Input ("fundamental soliton") and output pulses after collision with 3, 6, and 9 resonant DWs (all curves shifted to $t = 0$ for better comparison).

achieved with segments of the continuum containing more energy.

6 Criteria for rogue waves

In [18] it has been demonstrated that giant solitons generated by acceleration fulfill the generally accepted main criteria for rogue waves, namely their heavy-tail amplitude distribution, their unpredictability, and the appearance of events that significantly exceed the average wave height. See [43] for a detailed discussion. In the following, we want to provide a more detailed discussion of criteria which have been brought up. These criteria are discussed in their order of importance as in [43], with the original citation marked in italics.

1. In the science of ocean waves, there was a suggestion to call a wave "rogue" if its amplitude is more than twice (or 2.5 times) that of the average amplitude of the significant wave height. With some restrictions, this definition can be extended to other fields as well. In our research we observe peak amplitudes that exceed the average wave crest by up to a factor 5 [18]. In fact, in this sense optical rogue waves are more roguish than their ocean analogues.

2. Another important feature of a rogue wave is its unpredictability. Figuratively speaking, a rogue wave is a wave that "appears from nowhere and disappears without a trace". Thus, to a large extent, the phenomenon is chaotic. Fundamental solitons have often been excluded as possible candidates for rogue waves as they are stable and may therefore not simply disappear. However, once the soliton is driven towards the zero-dispersion wavelength, this paradigm becomes shattered. When driven beyond this critical wavelength, the soliton will immediately decay. At the verge of this critical condition, soliton parameters may vary dramatically according to input conditions, which, in turn, dramatically affect the peak power of the resulting soliton.

3. The third feature is related to the probability distribution function (PDF) of the wave amplitudes. Namely, large waves appear much more often than they would according to Gaussian

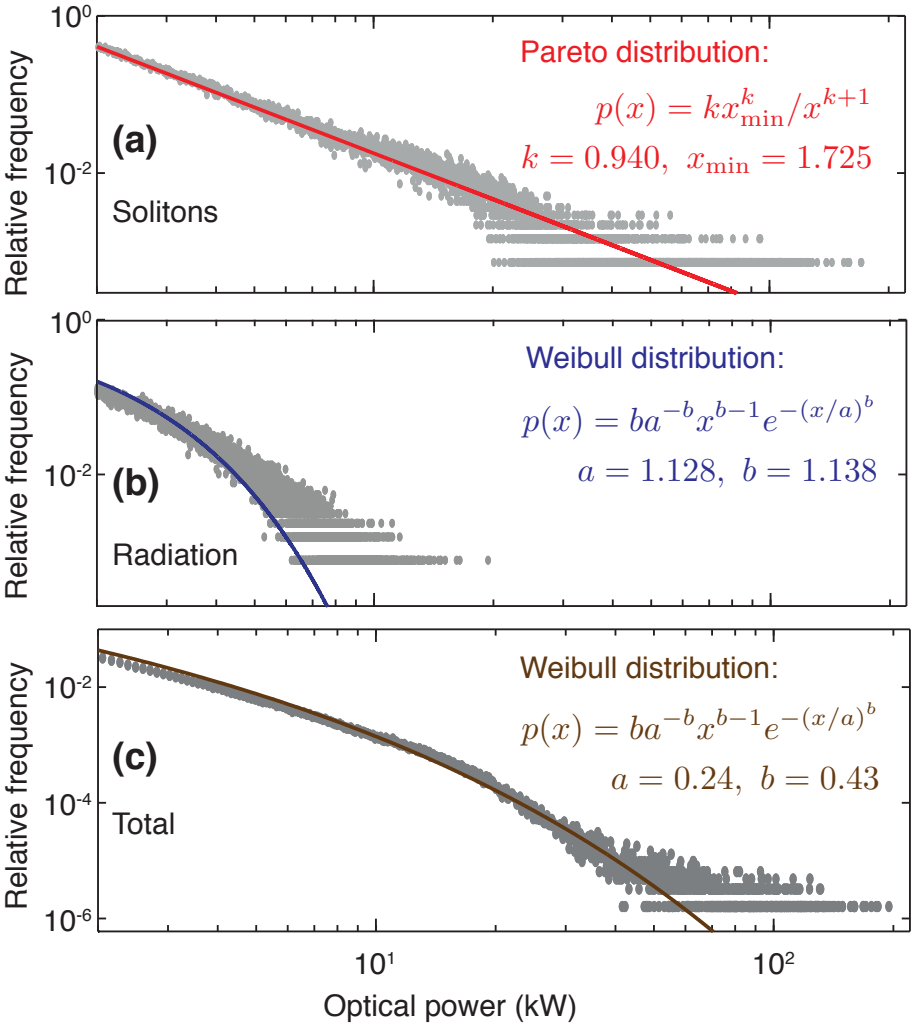

Figure 8: Statistical distribution on a log-log scale for (a) the anomalous dispersion regime with a fit to a Pareto distribution, (b) the normal dispersion regimen with a fit to a Weibull distribution, and (c) the whole spectrum without filtering of any kind with a fit to a Weibull distribution.

statistics. Experimental studies on rogue waves usually produce elevated tails of the PDF. The heavy-tailed probability of rogue waves, which is typical for rare-but-extreme events, has been demonstrated for the fiber supercontinuum scenario using a spectral filter [35, 46], yet also without such filtering [35, 18] as filtering may produce misleading results [48].

As filtering obviously plays an important role, we have extracted separate statistics from our simulation results. Figure 8 present the statistics (a) for the anomalous regime, (b) the normal dispersion regime, and (c) the whole spectrum without filtering of any kind. This analysis clearly reveals a deviation from a Gaussian distribution. However, we observe another interesting feature. The long tail behavior for the dispersive waves differs from that of the solitons. In [47] it has been observed that collisions between solitons create giant dispersive waves. In our case, however, we cannot attribute the dispersive waves with high peak powers solely to soliton-soliton collisions.

4. Is the phenomenon of "rogue waves" linear or nonlinear? Present approaches are inclined to the version of their nonlinear nature. Indeed, linear theories of rogue waves can only produce Gaussian PDFs, so the appearance of large waves would have very small probability. In our case, the presented phenomenon is clearly nonlinear.

5. What is the onset of appearance of "rogue waves"? Is the phenomenon related to modulation instability? The latter question was first posed by Peregrine in his paper of 1983 in relation to ocean waves. There is little doubt that one or other form of instability is indeed responsible for generating large waves. The supercontinuum generation process as modeled here is fully capable of producing a modulation instability [41, 40]. It manifests itself via certain periodic spikes at the beginning of the supercontinuum generation process. It is known that the MI can initiate soliton fission, but is not a necessary prerequisite for the fission process [44]. This finding is also demonstrated in Fig. 2 and Fig. 3.

6. How does the spectral content of a wave field evolve in order to produce a rogue wave? In optics, as well as in other fields like capillary waves, the spectral content starts with a single or narrow spectral component that spreads, first into a triangular spectrum shape, while then later it creates a so-called "supercontinuum". In one form or other, this happens in other fields too. Here the described rogue wave formation in the supercontinuum generation process requires two different wavelengths, which can widely be separated. Therefore extremely broad spectra have to be considered for their observation.

7 Conclusion

Here we discussed a new mechanism that contributes to rogue wave formation in optical fiber supercontinua. This mechanism relies on interaction between a dispersive wave in the normal dispersion regime and a soliton in the anomalous dispersion regime. The mechanism proposed here does not presuppose any special nonlinear effects that are unique to optical systems. In comparison to previously discussed mechanisms of rogue wave formation, our approach essentially only presupposes a nonlinear Schrödinger type scenario, with a reactive nonlinearity and a concave dispersion profile, the latter enabling copropagation of radiation with opposite signs of dispersion with equal group velocity. Suitable conditions are found in a variety of physical systems and also outside optics, e.g., for gravity-capillary waves [49]. Our explanation is therefore immediately applicable to a wider class of physical systems. We therefore believe that the previously disregarded scattering of DWs and solitons provides new insight in the fascinating appearance of extreme-value wave phenomena in a multitude of physical scenarios.

References

[1] K. Dysthe, H. E. Krogstad, and P. Müller, Annu. Rev. Fluid Mech. **40**, 287 (2008).

[2] A. N. Ganshin *et al.*, Phys. Rev. Lett. **101**, 065303 (2008).

[3] Yu. V. Bludov, V. V. Konotop, and N. Akhmediev, Phys. Rev. A **80**, 033610 (2009).

[4] M. S. Ruderman, Eur. Phys. J. Special Topics **185**, 57 (2010).

[5] L. Stenflo and M. Marklund, J. Plasma Phys. **76**, 293 (2010).

[6] D. R. Solli *et al.*, Nature **450**, 1054 (2007).

[7] J. Kasparian *et al.*, Opt. Express **17**, 12070 (2009).

[8] D. Majus *et al.*, Phys. Rev. A **83**, 025802 (2011).

[9] C. Kharif and E. Pelinovsky, Eur. J. Mech. **22**, 603 (2003).

[10] P. A. E. M. Jannsen, J. Phys. Oceanography **33**, 863 (2003).

[11] M. Onorato *et al.*, Phys. Rev. Lett. **86**, 5831 (2001).

[12] A. Mussot *et al.*, Opt. Exp. **17**, 1502 (2009); M. Taki *et al.*, Phys. Lett. A **374**, 691 (2010).

[13] D. R. Solli, C. Ropers, and B. Jalali, Phys. Rev. Lett **101**, 233902 (2008).

[14] J. M. Dudley, G. Genty, B. J. Eggleton, Opt. Exp. **16**, 3644 (2008); M. Erkintalo, G. Genty, and J. M. Dudley, Opt. Lett. **35**, 658 (2010); G. Genty, J. M. Dudley, B. J. Eggleton, Appl. Phys. B **94**, 187 (2009).

[15] N. Akhmediev, J. M. Soto-Crespo, and A. Ankiewicz, Phys. Rev. A **80**, 043818 (2009); N. Akhmediev, A. Ankiewicz, and M. Taki, Phys. Lett. A **373**, 675 (2009).

[16] N. Akhmediev, A. Ankiewicz, and J.M. Soto-Crespo, *Phys. Rev. E* **80**, 026601 (2009).

[17] B. Kibler *et al*. Nature Physics **6**, 790 (2010).

[18] A. Demircan, Sh. Amiranashvili, C. Brée, C. Mahnke, F. Mitschke, and G. Steinmeyer, Sci. Rep. **2**, 850 (2012).

[19] Smith, R. Reflection of short gravity waves on a non-uniform current. *Math. Proc. Camb. Phil. Soc,* **78**, 517-Ű525 (1975).

[20] C.M. De Sterke, Opt. Lett. **17**, 914 (1992).

[21] N. Rosanov, JETP Lett. **88**, 501 (2008).

[22] V.E. Lobanov, and A.P. Sukhorukov, Phys. Rev. A **82**, 033809 (2010).

[23] A. V. Gorbach, and D. V. Skryabin, Opt. Express, **15**, 14560 (2008).

[24] D.V. Skryabin and A.V. Gorbach, Rev. Mod. Phys. **82**, 1287 (2010).

[25] Novello, M., Visser, M. & Volovik, G. (eds.) Artificial Black Holes. (World Scientific, New Jersey, London, Singapore, Hong Kong, 2002).

[26] T. G. Philbin, C. Kuklewicz, S. Robertson, S. Hill, F. König, & U. Leonhardt, Science **319**, 1367 (2008).

[27] D. Faccio, Cont. Phys. **1**,1 (2012).

[28] G. Agrawal, *Nonlinear Fiber Optics* (Academic Press, San Diego, 2001).

[29] L. J. Garay, J. R. Anglin, J. I. Cirac, & P. Zoller, Phys. Rev. Lett. **85**, 4643 (2000).

[30] T. A. Jacobson, & G. E. Volovik, Phys. Rev. D **58**, 064021 (1998).

[31] F. Belgiorno, S. L. Cacciatori, M. Clerici, V. Gorini, G. Ortenzi, L. Rizzi, E. Rubino, V. G. Sala, & D. Faccio , Phys. Rev. Lett. **105**, 203901 (2010).

[32] G. Rousseaux, C. Mathis, P. Maïssa, T. G. Philbin, & U. Leonhardt, New J of Phys. **10**, 053015 (2008).

[33] R. Driben, F. Mitschke, and N. Zhavoronkov, Opt. Exp. **18**, 25993 (2010).

[34] V. E. Zakharov, E. Pushkarev, V. F. Shvets, and V. V. Yan'kov, JETP Lett. **48**, 83–87 (1988).

[35] G. Genty *et al.*, Phys. Lett. A **374** 989 (2010).

[36] Sh. Amiranashvili and A. Demircan, Phys. Rev. A **82**, 013812 (2010).

[37] Sh. Amiranashvili and A. Demircan, Adv. Opt. Tech., **2011**, 989515 (2011).

[38] J. Herrmann *et al.*, Phys. Rev. Lett. **88**, 173901 (2002).

[39] Sh. Amiranashvili, U. Bandelow, A. Mielke, Opt. Commun. **283**, 480 (2009).

[40] A. Demircan and U. Bandelow, Opt. Comm. **244**, 181 (2005).

[41] J. M. Dudley, G. Genty, S. Coen, Rev. Mod. Phys. **78**, 1135 (2006).

[42] R. Driben, I. Babushkin, Opt. Lett. **37**, 5157 (2012).

[43] N. Akhmediev, and E. Pelinovsky, Eur. Phys. J. Special Topics **185**, 1 (2010).

[44] A. Demircan and U. Bandelow, Appl. Phys. B **86**, 31 (2007).

[45] A. Demircan, Sh. Amiranashvili, G. Steinmeyer, Phys. Rev. Lett. **106**, 163901(2011).

[46] B. Kibler, K. Hammani, C. Michel, Ch. Finot, and A. Picozzi, Phys. Lett. A **375**, 3149 (2011).

[47] M. Erkintalo, G. Genty, and J. M. Dudley, Opt. Lett. **35**, 658 (2010).

[48] M. Erkintalo, G. Genty, and J. M. Dudley, Eur. Phys. J. Special Topics **185**, 135 (2010).

[49] H. Lamb, *Hydrodynamics* (6th ed.), Cambridge University Press (1994).